18th Australasian Fluid Mechanics Conference
Launceston, Australia
3-7 December 2012

Direct Numerical Simulation of Periodic Streaming around a Circular Cylinder at Low *KC* Number and Low β Number

H. An[1], L Cheng[1] and M. Zhao[2]

[1] School of Civil and Resource Engineering
University of Western Australia, Crawley, Western Australia 6009, Australia

[2]School of Computing, Engineering and Mathematics
University of Western Sydney, Penrith New South Wales 2751, Australia

Abstract

Sinusoidal oscillatory flow around a circular cylinder is simulated to study the periodic streaming in three flow regimes under the low *KC* and low β number conditions. The first regime of periodic streaming is featured by V-shape jet-like streams towards a fix direction. In the second regime, the V-shaped streams also exist, but the V-shape switches direction with a secondary flow period. The third regime is characterized by a helical-blade-shaped streaming structure. Periodic streaming has significant effects on mass/momentum/energy transfer around a cylinder in oscillatory flow.

Introduction

The sinusoidal oscillatory flow around a circular cylinder or a circular cylinder oscillating in a viscous fluid otherwise at rest has been of significant academic and practical interests. An oscillatory flow is defined as $u(t) = U_m\sin(2\pi t/T)$, where U_m is the velocity amplitude of oscillatory flow and T is the period of oscillatory flow. The characteristics of oscillatory flow around a circular cylinder are governed by two parameters: Keulegan-Carpenter number ($KC = U_mT/D$) and Frequency number ($\beta = D^2/\nu T$), where D is the diameter of the cylinder and ν is the kinematic viscosity of fluid.

Steady streaming is one of the most important flow phenomena of oscillatory flow around a circular cylinder. Steady streaming represents the temporally averaged flow field around the cylinder. It has been of great interests in the area of hydrodynamics and acoustics. Most of the previous research work about steady streaming was carried out under the condition of small amplitude and high-frequency oscillations where analytic solution of steady streaming was achievable or steady streaming can be observed directly in experiments ([1], [2] and [3]). Most of the work about steady streaming under high frequency small amplitude oscillations has been summarized in several review papers ([4], [5]).

Steady streaming also exists under high *KC* conditions (large amplitude oscillation). Liang and Cheng [6] investigated local scour below a submarine pipeline numerically and observed steady streaming in the vicinity of the pipeline throughout the scour process ($KC = 11$, $Re = 7000$). An et al. [7] carried out a two-dimensional numerical simulation in the range of $2 \le KC \le 40$ ($\beta = 196$) and identified six different steady streaming structures corresponding to different oscillatory flow regimes.

The above mentioned work was all carried out under two-dimensional flow conditions. It has been known that flow only maintains as two-dimensional under very low *KC* and low β conditions. Tatsuno and Bearman [8] performed a flow visualization study in the range of $0 < KC < 15$ and $0 < \beta < 150$. Eight flow regimes (named as A*, A, B, C, D, E, F and G) were classified according to the features of the flow. The flow is three-dimensional in most of the regimes except for regime A* and A. In regime A and A*, the steady streaming is comprised of four inner circulating cells and four outer cells in a symmetric pattern with respect to the *x*- and *y*-axes ([1] and [2]). The three-dimensional flow structure in regime B is named as Honji vortex or Honji instability [9]. This is characterized by mushroom-shaped vortices around the cylinder. Honji instability (regime B) related steady streaming has been explored by An et al. [10] using direct numerical simulations (DNS).

When the oscillatory flow around a cylinder is aperiodic, the steady streaming needs to be calculated over a large number of flow periods to obtain a converged flow pattern. An et al. [10] demonstrated that at $KC = 2$ and $\beta = 500$, the average of flow velocity over 80 flow periods gave a converged steady streaming structure. It was demonstrated that three dimensional flow features were unfortunately filtered out in the converged flow and the steady streaming became almost two-dimensional.

In this work, the average of flow over one flow period is defined as periodic streaming (PS). It is identical to steady streaming when the flow is periodic, but it is different when flow changes from period to period. This definition gives the averaged flow information without losing the intrinsic three-dimensional features.

The present research aims at exploring the three-dimensional PS in regime D, E and F.

Governing equations

In this study, sinusoidal oscillatory flow around a fixed circular cylinder is simulated numerically. The governing equations are the non-dimensional Navier-Stokes equations and the continuity equation. The governing equations in Cartesian coordinate system (shown in Figure 1) are given as:

$$\frac{1}{KC}\frac{\partial u_i}{\partial t} + u_j\frac{\partial u_i}{\partial x_j} + \frac{\partial p}{\partial x_i} - \frac{1}{KC\beta}\frac{\partial^2 u_i}{\partial x_j^2} = 0 \quad (1)$$

$$\frac{\partial u_i}{\partial x_i} = 0 \quad (2)$$

where u_i represents velocity component in the x_i-direction and p is the pressure.

A non-slip boundary condition is given on the surface of the cylinder. On the inlet boundary, velocity is specified as:

$$(u, v, w) = (U_m\sin(2\pi t/T), 0, 0) \quad (3)$$

And pressure condition is specified according to $\partial u/\partial t \approx \partial p/\partial x$. At the outflow boundary, the pressure is set to be zero and velocity gradients in the flow direction are set to zero. A periodic boundary condition is used on the two boundaries in the

axial direction of the cylinder. A free slip boundary condition is implemented on the two side boundaries.

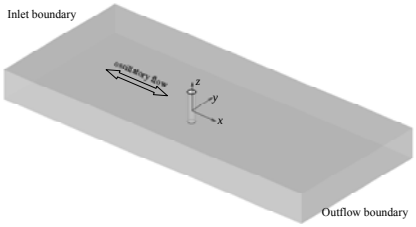

Figure 1. Coordinate system and computational domain.

Numerical Methods

The Petrov-Galerkin finite element method is employed for discretizing the Navier-Stokes equations. In the Petrov-Galerkin formulation the standard Galerkin weighting functions are modified by adding a streamline upwind perturbation, which acts only in the flow direction. Details about the finite element discretization can be found in Zhao et al. [11]. The parallel computing program code based on message passing interface (MPI) is developed for the calculations.

A definition sketch of the coordinate system is shown in Figure 1. The flow oscillates along the *x*-axis direction. Eight-node hexahedral elements are employed to discretize the three-dimensional domain. Three DNS are carried out with (KC, β) = (6, 25), (5, 45) and (8, 25), which correspond to regime D, E and F, respectively. The domain dimensions used in the first two cases are 60D, 30D and 10D in the *x*-, *y*- and *z*-axis directions, respectively. The cylinder circumference is discretized by 96 nodes. The minimum element size in the radial direction next to the cylinder surface is 0.001D. Spanwise mesh size is 0.1D. The total node number is 608,190 and total mesh element number is 587,520. In the third case (for regime F), a larger cylinder length of 16D is used to resolve large spanwise structures which were observed experimentally [8]. The domain size and mesh density in the *x* and *y* directions are the same as those used in the first two cases. The computational time for each case was about 12 days with 16 of the 1600 CPUs on an iVEC 87.20 TeraFLOPS supercomputer.

In this study, the PS is defined as the averaged flow field over one flow period. The PS velocity ($\bar{u}_i, i = 1,2,3$) is calculated as:

$$\bar{u}_i = \int_{t_0}^{t_0+T} u_i \, dt \qquad i = 1, 2, 3 \tag{4}$$

where t_0 is an arbitrary instant after the flow has been fully developed.

Numerical Results

Regime D

Regime D happens along a narrow range bounded by regime A and E in the KC-β regime map marked by Tatsuno and Bearman [8]. The flow breaks symmetry along the *x*-*z* plane and two vortex streets form a V-shape. The wave length of the three-dimensional flow structure along the spanwise direction is 3D ~ 5D.

To study the PS in regime D, the flow with KC = 6 and β = 25 was simulated for 200 periods. To detect the development of three-dimensionality, two probe lines with x = 0 and y/D = ±0.51 were set during the numerical simulation to record the flow velocity. The spanwise flow velocity along x = 0 and y/D = -0.51 corresponding to the peak free stream velocity in 200 flow periods is plotted in Figure 2, where N represents the number of flow periods. The figure shows that flow remained as two-dimensional in the first 50 periods and then three-dimensional flow structures emerged. Each pair of blue-red strips corresponds to one three-dimensional vortex comprising of a pair of counter-rotating vortices. From the 50th to the 90th periods, three three-dimensional vortices were observed to be distributed uniformly along the spanwise direction. After the 90th periods the three-dimensional vortices become unstable. At about the 135th period, the blue strip from the top and the red strip from the bottom of the figure slid along the cylinder and formed a new pair in the middle. After that, the tracks of three-dimensional vortices show obvious wavy features. The spanwise velocity detected along the line of x = 0 and y/D = 0.51 is always zero during the 200 flow periods. This feature demonstrates that the V-shape vortex street is always towards the same direction.

The PS is calculated based on the flow in the 145th flow period and the corresponding three-dimensional streamlines are plotted in Figure 3. The three-dimensional streamlines show the existence of three pairs of straight jet-like streams shooting out from the two sides of the cylinder. The streamlines are symmetric with respect to the plane of x = 0. The shooting streamlines can be fitted by

$$y/D = \pm 0.7x/D - 0.6 \tag{5}$$

The angle between the pair of streams is 110°. The spanwise distance between two streams is 3.33D, which falls in the range observed by Tatsuno and Bearman [8]. It should be noted that the spanwise distance is dependent on the domain length in z-direction due to the nature of periodic boundary conditions applied. Since the number of three-dimensional vortices in the computational domain will always be an integer, the longer the domain length in z-direction the more accurate prediction of the spanwise distance. Figure 3 also shows that three-dimensional flow structures only exist around the shooting streams. In between two pairs of streams, the flow structure only shows very weak three-dimensionality.

Figure 4 (a) show the flow structure in the *x*-*y* plane of z/D = 0, which cuts through the middle of the pair of shooting streams shown in Figure 3. Streamlines and contours of velocity magnitude ($=\sqrt{\bar{u}^2 + \bar{v}^2 + \bar{w}^2}$) are plotted. The shooting streams extend about 10D away from the cylinder. The maximum streaming velocity is 46.5% of U_m.

Figure 4 (b) shows a zoom-in view of the flow structure in the plane of z/D = 0. Three streamlines are plotted on each side of the cylinder. The streamlines swirl around the cylinder in the plane but do not form closed loops and exit from the computational domain, indicating the three-dimensionality of the flow structure. All streamlines shoot out from the lower side of the cylinder and form the two strong streams. Figure 4 (c) shows the flow structure in the plane of z/D = 1.67, which is in between two pairs of shooting streams. The pattern of streamlines is similar to that shown in Figure 4 (a), but without the strong shooting streams. A zoom-in view of the flow structure is given in Figure 4 (d), where four circulating cells are formed around the cylinder with larger cells on the lower side of the cylinder. The maximum PS velocity is 40% of U_m. Similar flow structure exists at other locations between the two pairs of shooting streams.

The above description is the typical feature of the PS in the Regime D. The PS calculated from other flow periods may exhibit minor differences due to the variation of the positions of vortices along the cylinder.

The flow structure shown in Figure 4 shows a strong correlation with the observation of particle distribution in the test reported by Tatsuno and Bearman (Figure 17 in reference [8]). This demonstrates that PS has significant contribution to the transport of mass around the cylinder. In the same way, it will affect momentum/energy transfer around the cylinder.

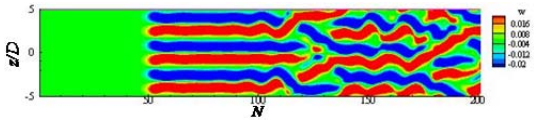

Figure 2. The spanwise flow velocity distribution along line of $x = 0$ and $y/D = -0.51$ corresponding to peak free stream flow ($KC = 6$ and $\beta = 25$).

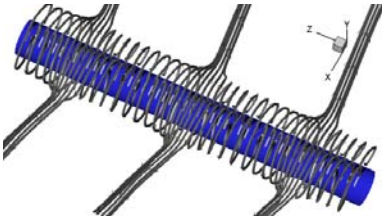

Figure 3. PS of regime D represented by three-dimensional streamlines ($KC = 6$ and $\beta = 25$).

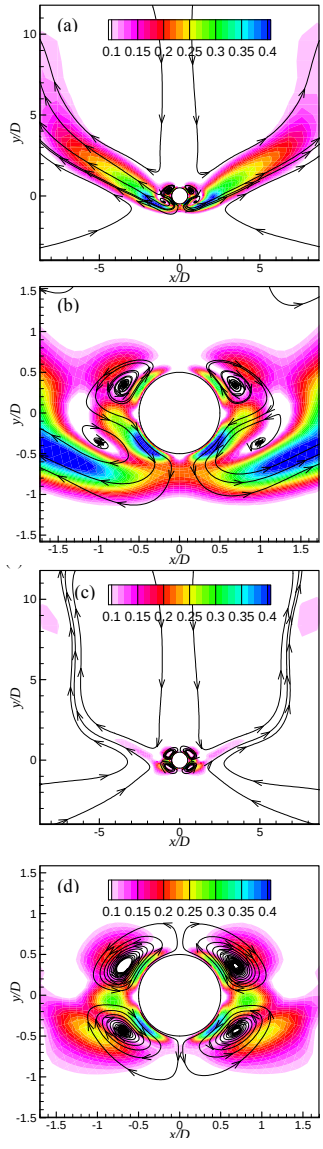

Figure 4. Streamlines and velocity magnitude contours in the plane of $z/D = 0$ (a, b) and $z/D = 1.67$ (c, d) in case of $KC = 6$ and $\beta = 25$ (regime D).

Regime E

Oscillatory flow switches from Regime D to regime E with the increase of β. The V-shape vortex street also happens in regime E. The distinguishable feature of regime E is that the V-shape vortex street switches to the opposite side occasionally according to the observation of Tatsuno and Bearman [8]. To study PS in regime E, a case with $KC = 5$ and $\beta = 45$ was simulated for 200 periods. The spanwise direction velocity detected along lines of $x = 0$ and $y/D = \pm 0.51$ is plotted in Figure 5. Three-dimensional instability initiates from the negative y side of the cylinder with three pairs of red-blue strips shown in Figure 5 (b) from 60 to 95 periods. Meanwhile the velocity at the positive y side shows featureless two-dimensionality. From the 95 period, the vortex structures become unstable. Firstly, all the three pairs of strips switch to the opposite side of the cylinder, as shown in Figure 5 (a) around the 100th period, then the strips in Figure 5 become non-parallel to the horizontal axis due to two reasons. One is that the three-dimensional flow structures switch direction at different times. The other reason is that the three-dimensional structures slid along the spanwise direction for $N > 105$, where N is the number of flow periods.

Figure 5 shows that there is a secondary flow period (about 15T to 20T). Elston et al. [12] investigated the instability of oscillatory flow around cylinder under low KC and low β number conditions using DNS and Floquet method. It was pointed out that secondary flow period is mainly a function of β and a secondary flow period of 15T at $\beta = 45$ was predicted. The present numerical results are in reasonable agreement with the Floquet analysis of Elston et al [12].

The PS calculated from the 80th and 120th flow periods is plotted in Figure 6 which shows three pairs of streams shooting out towards positive y direction in the 80th period and switches to the negative direction at the 120th period. The flow structure in the x-y plane is similar to that shown in Figure 4 and no more detail is given here.

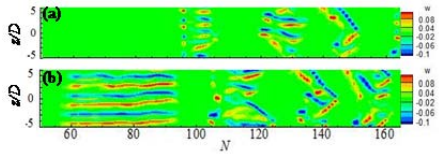

Figure 5. The spanwise flow velocity distribution along two lines at peak free stream flow ((a) $x/D = 0$ and $y/D = 0.51$. (b) $x/D = 0$ and $y/D = 0.51$. $KC = 5$ and $\beta = 45$).

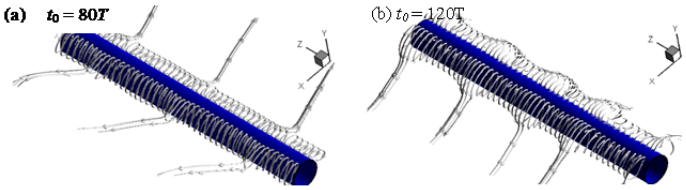

Figure 6. PS of regime E represented by three-dimensional streamlines ($KC = 5$ and $\beta = 45$).

Regime F

According to the observation of Tatsuno and Bearman [8], in regime F, vortex shedding happens and forms an inclined vortex street with respect to the oscillatory direction of the cylinder. When the flow changes to three-dimensional, the spanwise scale of three-dimensional structure is in the range of 3.5D to 6D. To study PS in this regime, an oscillatory flow with $KC = 8$ and $\beta = 25$ was simulated for 200 periods. Since a large span length of the three-dimensional structure is anticipated, a computational domain of 16D is used. The flow changes to three-dimensional from the 50th period with four uniformly distributed spanwise structures. The four vortex structures remain stable in 200 flow periods.

Three-dimensional streamlines are plotted in Figure 7 to examine PS in this regime. Figure 7 (a) shows that the streamlines are distributed in an anti-symmetric pattern with respect to the z-axis.

The streamlines flowing out in the *x* direction are almost uniformly distributed, unlike the jet-like streams in regime D and E. A zoom-in view of a few streamlines is given Figure 7 (b). The starting points of the streamlines are close to the cylinder surface. Firstly all the streamlines are parallel and creep along the cylinder surface, then shoot out towards positive *y* direction. After that the streamlines separate into two groups, with one group flowing out towards positive *x* direction and the other group forming a circulating cell close to the cylinder. This is the typical flow pattern of PS in this flow regime.

Flow structure in the *x*-*y* plane of this case is examined. Figure 8 (a) shows the flow structure in the plane of $z/D = 0$, which cuts through the streamlines shooting out directly (Figure 7 (b)). The velocity magnitude of PS in this plane is up to about 33% of U_m around the cylinder. The contours of PS velocity magnitude are in the shape of a pair of helical blades, which extend more than 15*D* along the positive and negative *x* directions. The plane of $z/D = 2$ (Figure 8 (b)) cutting through the recirculating cell is shown in Figure 7 (b). The peak value of the velocity magnitude is about 0.47 U_m, much higher than the corresponding value in Figure 8 (a). Other than that, the shape of velocity contours and streamlines in Figure 8 (a) and (b) are very similar. This demonstrates that three-dimensionality in PS becomes weaker as further away from the cylinder.

Once again, PS structure shown in Figure 8 can explain the pattern of particle distribution in the work of Tatsuno and Bearman ([8], Figure 25).

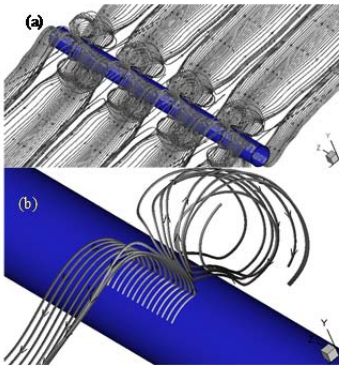

Figure 7. PS of regime f represented by three-dimensional streamlines ($KC = 8$ and $\beta = 25$).

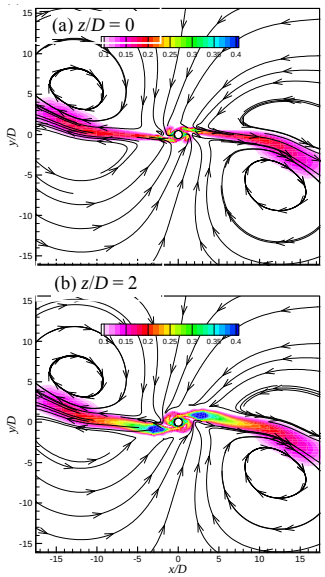

Figure 8. The typical PS structure of regime F represented by 3D streamlines (KC = 8 and β = 25).

Finial Remark

This paper reveals the PS in regime D, E and F defined by Tatsuno and Bearman [8] through a direct numerical simulation. In regime D, PS is in a V-shape towards the positive *y* direction. In regime E, PS is also in a V-shape, but it switches direction with a secondary flow period approximately 15~20T. In Regime F, PS is characterized by stable helical-blade shaped flow structure.

The PS presented in the present work can be used to explain the distribution of particles around a cylinder in oscillatory flow. PS has significant contribution to mass/momentum/energy transfer around a cylinder in oscillatory flow.

The three cases presented here uncover the main features of the PS in the three flow regimes. It is expected that variation of the PS still exists within certain flow regimes. More simulations are needed to understand the PS further.

Acknowledgments

The authors would like to thank iVEC for providing supercomputing facilities.

References

[1] Holtsmark, J., Johnsen, I., Sikkeland, T. and Skavlem, S., Boundary layer flow near a cylindrical obstacle in an oscillating incompressible fluid. *J. Acoust. Soc. Am* 1954, 26, 26-39.

[2] Wang, C.Y. On high-frequency oscillatory viscous flows. *J. Fluid Mech.* 1968, 32, 55- 68.

[3] Yan, B., Ingham, D.B. and Morton, B.R., Streaming flow induced by an oscillating cascade of circular cylinders. *J. Fluid Mech.* 1993, 252, 147-171.

[4] Lighthill, J. Acoustic streaming. *J. Sound Vibrat.* 1978, 61, 391-418.

[5] Riley, N. Steady Streaming. *Annu. Rev. Fluid Mech*. 2001, 33, 43-65.

[6] Liang, D.F. and Cheng L., Numerical model for wave-induced scour below a submarine pipeline. *J. of Waterway, port, Coastal Ocean Eng*, 2005, 131(5), 193-202.

[7] An, H., Cheng, L. and Zhao M. Steady streaming around a circular cylinder in an oscillatory flow. *Ocean Eng*. 2009, 36, 1089-1097.

[8] Tatsuno, M. and Bearman, P.W. A visual study of the flow around an oscillating circular cylinder at low Keulegan-Carpenter numbers and low Stokes number. *J. Fluid Mech*. 1990, 211, 157-182.

[9] Honji, H. Streaked flow around an oscillatory circular cylinder. *J. Fluid Mech*, 1981, 107, 509-520.

[10] An, H., Cheng, L. and Zhao M. Direct numerical simulation of oscillatory flow around a circular cylinder at low Keulegan–Carpenter number. *J. Fluid Mech*, 2011, 666, 77-103.

[11] Zhao, M., Cheng, L. & Zhou, T. Direct numerical simulation of three-dimensional flow past a yawed circular cylinder of infinite length. *J. Fluids Struct*. 2009, 25, 831–847.

[12] Elston, J. R., Blackburn, H. M. & Sheridan, J. The primary and secondary instabilities of flow generated by an oscillating circular cylinder. *J. Fluid Mech*. 2006, 550, 359–389.s